

RESEARCH ARTICLE

Performance enhancement of centrifugal pumps through axial clearance reduction: An experimental investigation

D. Satish^{1,2*}, A. Doshi¹, M. Bade¹

¹Department of Mechanical Engineering, Sardar Vallabhbhai National Institute of Technology, Surat 395007, Gujarat, India

²Department of Mechanical Engineering, Sarvajani College of Engineering and Technology, Surat 395001, Gujarat, India

Phone: +917359509403

ABSTRACT - It is a well-known fact that the disk friction phenomena due to axial clearance has a significant impact on centrifugal pumps performance. Enhancing the efficiency of centrifugal pumps is crucial, as these pumps are widely used in industries and contribute significantly to energy consumption, offering substantial potential for energy savings and cost reduction. In the present work, the disk friction due to the axial clearance between the impeller and the back cover plate was examined experimentally for three commercial centrifugal pumps with specific speeds, $N_s = 19, 34$ and 54 rpm at various flow rates. Hydraulic performance parameters were obtained for two different cases: one with original axial clearance and other with minimum axial clearance at rated/design (1450 rpm) and off-design (1000 rpm) conditions. In both conditions, pumps with minimum clearance provides the higher overall efficiency compare to the original clearance. At design conditions, $N_s = 34$ rpm, the result shows higher performance improvement compared to $N_s = 54$ rpm with efficiency rise of 5.20% . Although, the highest efficiency of 84.48% was obtained for $N_s = 54$ rpm at maximum flow rate. Similarly, significant rise in parameters were observed for $N_s = 34$ followed by $N_s = 19$ and $N_s = 54$ rpm at off-design conditions. Change in experimental disk friction head loss due to clearance reduction were compared to provide a clearer image about performance enhancement.

ARTICLE HISTORY

Received : 17th Dec. 2024
Revised : 28th Feb. 2025
Accepted : 02nd Mar. 2025
Published : 30th June 2025

KEYWORDS

Commercial pumps
Axial clearance
Disk friction loss
Design and off-design
Specific speed

1. INTRODUCTION

A form of general rotating machinery, centrifugal pumps are employed in a wide range of industries, such as irrigation of agricultural land, water drainage, and water delivery. A centrifugal pump employs the centrifugal force produced by the impeller's rotation to move the fluid. Centrifugal pumps are widely used in several industries, including the coal, construction, power generation, and water sectors, for the movement of slurries that contain solid particles. Research and development as well as the production of centrifugal pumps are growing rapidly. Among the all end user energy sectors, industries are the major energy consumer (~38% of total final consumption) and highest Carbon Dioxide (CO₂) emitter (~47% of total emission) by 2023 [1]. Figure 1 depicts the industrial electricity demand in 2022 by various end users. It also provides the future statistics by 2030 and 2050 for Stated Policies Scenario (STEPS), Announced Pledges Scenario (APS) and Net Zero Emissions (NZE) levels [1]. In modern industries, motor-driven devices consume about 65% of the electricity used in the sector in 2022. Drives for pumps, fans, material handling, processing, compressed air systems, and other applications are run by motors. Almost 60% (630 tera watthours [TWh]) of the increase in electricity demand over the past ten years has come from motor-driven systems, and in the years to come, they will likely account for most of the supply of electricity needed in the industry sector in all energy levels.

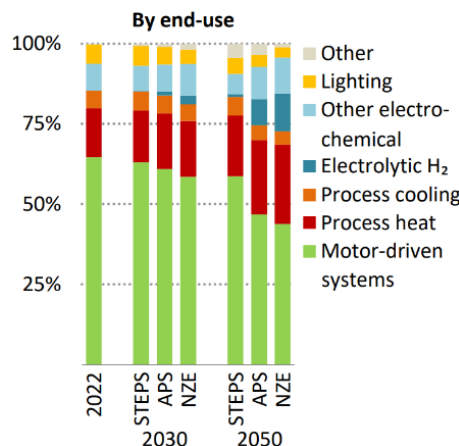


Figure 1. Industrial electricity demand by various end users [1]

As per Figure 2, one can see that pumps accounts for more than 24% of the energy used by industrial motor-driven systems. Furthermore, over 50% of the potential energy savings from motor powered pumps can be attributed to duty cycle fluctuation, Affinity Laws, and frequent oversizing of pump systems as depicted in Figure 3. This emphasises how important it is to concentrate on increasing pump efficiency. To facilitate this, the European Commission created the eco design specifications for water pumps in 2012. The overall energy usage of all pump systems in 2015 was recorded as 225 TWh/year in the expanded European Union report that was published in 2018 [2]. This estimate projects that by 2030, the yearly energy usage of water pumps would amount to 261 TWh. This energy-saving potential has a significant impact on the development of a new generation of energy-efficient pumps and pump systems. Nevertheless, several governmental and regulatory organizations are attempting to establish benchmarks for the development of energy-saving pumps.

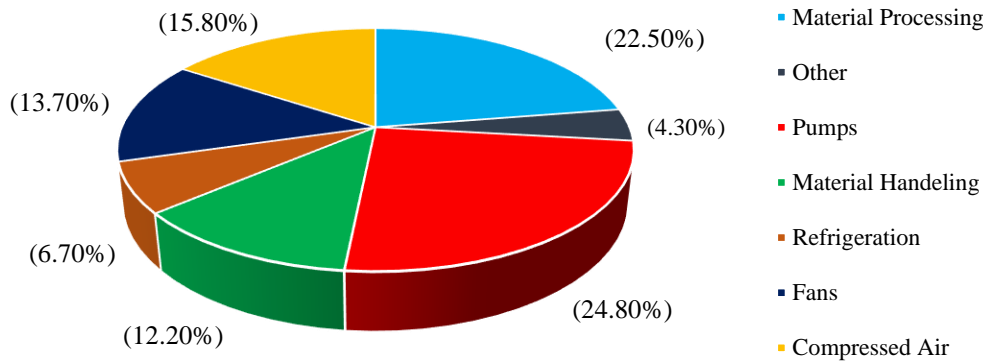


Figure 2. Industrial motor-driven systems energy usage (reconstructed) [3]

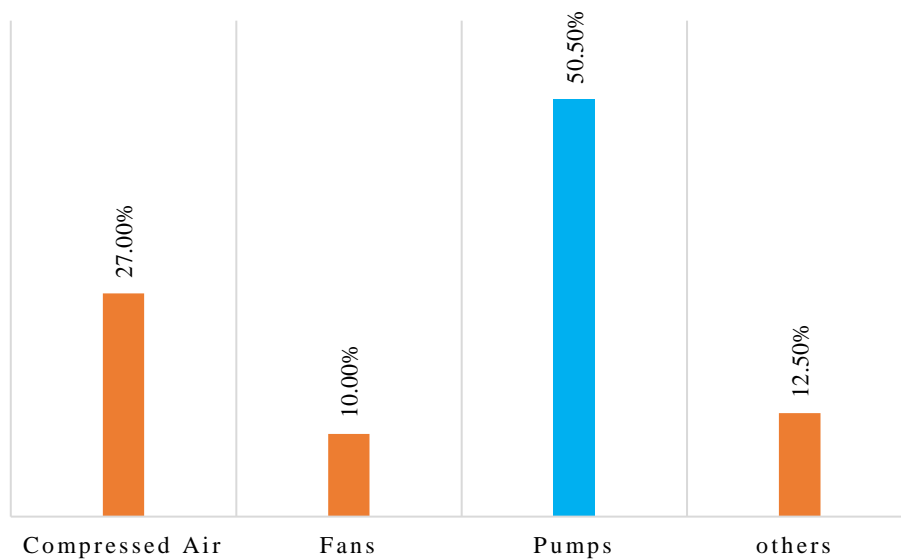


Figure 3. Industrial motor-driven systems energy saving potential (reconstructed) [3]

Due to the losses depicted in Figure 4, the centrifugal pump's output will always be less than its input power because it is an energy-operated device. There are essentially two categories for the pump losses: two types of losses: (1) external and (2) internal. The exterior losses that result from inadequate lubrication at the shaft and bearing seals are covered by mechanical losses. With the redesigned bearing, these losses can be minimized. Hydraulic losses and secondary losses are two more categories for internal losses. The fluid friction between the impeller and volute causes hydraulic losses to form in the pump's flow zone. The secondary losses are sub divided into the leakage losses due to the seal leakage and disk friction losses, DF_L due to the axial clearance, cl between the shrouds of the impeller and volute [4]. To reduce the hydraulic losses and leakage losses one needs to use highly smoothed impeller and volute. The location of each loss in pump where it occurred, the reason and its contribution in various types of losses are mentioned in Figure 4. All the remedies applied to reduce the mechanical as well as, hydraulic and leakage losses will add more cost and requires major modification in existing design of pumps. The DF_L can be reduced by lowering the cl using simple less costly methods which will not require major modification in pump design. Gülich [5] research highlights that DF_L have a significant impact on the efficiency of centrifugal pumps having low or moderate specific speed, N_s . For a low-speed pump ($N_s = 10$ rpm), DF_L typically accounted for about 50% of the useful power, whereas for high-speed pump ($N_s = 30$ rpm), this fraction was reduced to approximately 5%. Hence, further studies need to be done to reduce the DF_L on a pump having low N_s .

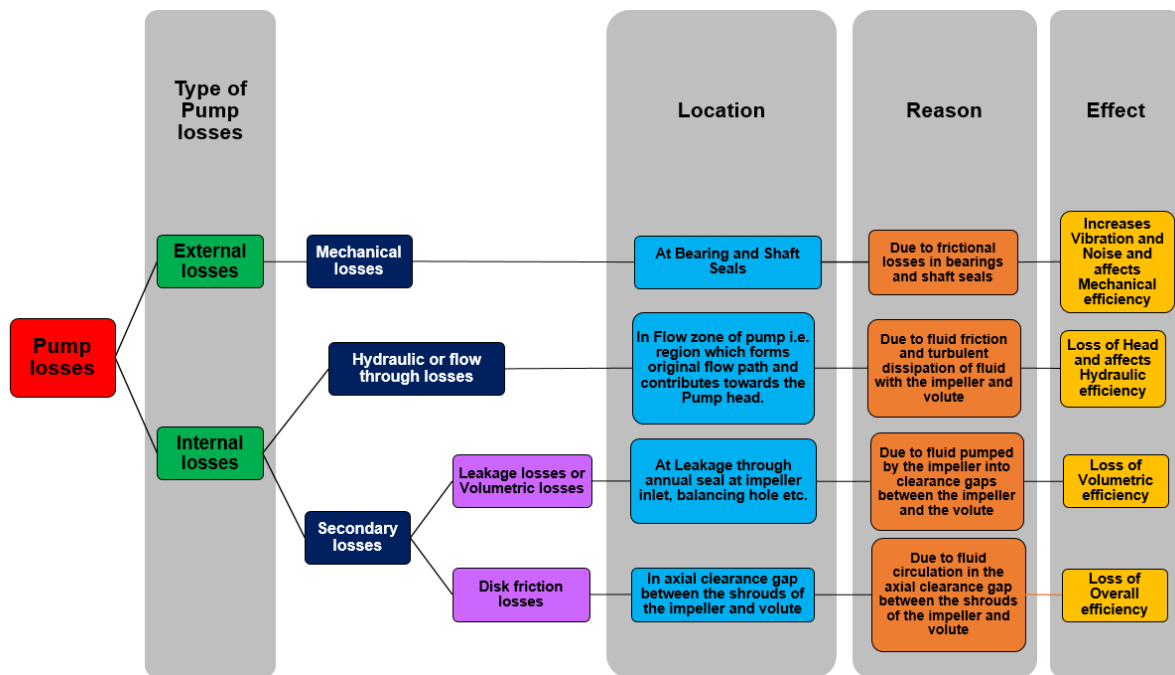


Figure 4. Pump losses – location, reason and effect

Various researchers have attempted to enhance the performance of centrifugal pumps by modifying the impeller geometry [6-8]; profile, angle and geometry of blades [9-11]; geometry of side channels as well as other geometrical parameters. A very few authors have explored the impact of reducing cl on DF_L [6, 12-14]. Will et al. [15] experimentally and numerically studied the flow dynamics of a moderate speed ($N_s = 22.8$ rpm) centrifugal pump using balancing holes. Their study found that balancing holes reduces the pressure gradients and axial force, F by introducing centripetal inward flow, which diminishes recirculation in the rear impeller clearances, cl . Ayad et al. [16] investigated the effect of cl on high speed centrifugal pump of $N_s = 28.7$ rpm performance using numerical simulations. They found that reducing cl by 3 mm improves the total head, H_T from 3.15 m to 5.9 m, overall efficiency, η_o from 40% to 47% and slip factor from 0.7 to 0.84. Similarly, Cao et al. [17] studied the effects of varying cl by 0.20 mm for a centrifugal pump of $N_s = 45.2$ rpm through model tests and simulations. Simulation results show that for each increment of 0.20 mm in cl , reduces η_o by 4.67%. Pehlivan and Parlak [18] simulated the effect of cl , wear ring and balancing holes on a single suction closed centrifugal pump with $N_s = 22.6$ rpm. Compared to the 51.5% η_o at 40 mm cl , the rise in η_o of 46.2% was obtained at 5 mm cl . Adistiya and Wijayanta [19] demonstrated that cl directly influences recirculation flow within a pump, affecting rotor stability, shaft integrity, and overall performance. Their calculations revealed that reducing cl from 0.02025 inches to 0.020 and 0.019 inches improved hydraulic efficiency, η_h from 28% to 29% and 36%, respectively, highlighting that smaller cl enhances the hydraulic performance. Streamline and pressure distribution in a $N_s = 24.7$ rpm centrifugal pump for with and without cl were examined using $k-\omega$ turbulence model by Zheng et al. [20]. In the volute, reducing the cl led to a lower pressure with a decrease in pressure fluctuation amplitude by 56.38% to 65.34%. Inaba et al. [21] investigated the effect of narrowing cl and reducing DF_L on the flow structure of a centrifugal pump impeller using an experimental and computational approach. Each approach supports that the vortex in the cl has a remarkable effect on reducing the DF_L under slightly inward flow conditions. Jin et al. [22] examined the influence of cl , flow rate, Q and impeller rotational speed (N) on DF_L using F for a centrifugal pump ($N_s = 23.4$ rpm). The outcome indicates that by reducing the cl from 0.5 mm to 0.1 mm, it greatly lowers the DF_L as F increases by nearly 74%. Peng et al. [23] studied the effect of varying cl (0.10, 0.22, 0.42 and 0.62 mm) on the hydraulic performance of $N_s = 45.2$ rpm centrifugal pump. Results found from the numerical simulations indicates that reducing cl from 0.62 mm to 0 mm, leakage flow rate from the volute into the front pump cavity reduces by 52.87% and from the front pump cavity back to the impeller inlet by 66.21%. The volumetric loss performance numerical analysis of a low speed ($N_s = 18.2$) pump was done by Kim et al. [24] using water as well as various viscosity crude oils for varying cl from 0.25 to 1.00 mm. Volumetric loss decreases with smaller cl , dropping from 0.0023 kg/s at 1 mm to 0.0015 kg/s at 0.25 mm for viscous fluids. To assess DF_L and internal flow of the clearance flow channel, Maeda et al. [25] numerically investigated the clearance flow channel, which replicates the clearance flow on the rear of the centrifugal impeller by utilizing rotating disks in a closed chamber. Results showed that the fin reduced DF_L by separating the clearance flow and increasing the circumferential velocity. Recently in 2024, Dokiparti et al. [26] have examined the effect of reduction in cl experimentally and numerically for $N_s = 54$ centrifugal pump. They found that reducing the cl from 13 mm to 1 mm enhances the η_o by 2.70% and 3.30% at rated 1450 and 1000 rpm, respectively.

The available literature survey indicates that by reducing the DF_L by lowering the cl , pump performance can be improved significantly using less costly means and minor modifications in pump design. Several experimental and numerical tests have been conducted on centrifugal pumps to reduce clearance. The pumps chosen in the majority of

studies are specially designed for the study, for example, with small pipes, lengthy diffusers, or specially profiled inlets. When evaluating the impact of clearance on commercial pumps, where the fluid enters the volute straight from the impeller, these results are unreliable. Therefore, the main objective of this research is to investigate the effect of reduction in DF_L for various specific N_s commercial centrifugal pumps. In the article, three different specific $N_s = 19, 34$ and 54 rpm pumps were experimentally tested at rated/design (1450 rpm) and off-design (1000 rpm) conditions. Two different cases were considered for performance comparison: one with the original clearance and the other with the minimum clearance. The article is arranged in the following pattern: pump geometries and clearance-reducing ring details, as well as experimental test setup and procedure, are provided in Section 2. Section 3 presents a thorough discussion of the experimental results. The concluding remarks are presented in Section 4.

2. MATERIALS AND METHODS

2.1 Geometry of the Commercial Centrifugal Pumps and Clearance Reducing Rings

Three different specific $N_s = 19, 34, 54$ rpm single suction and volute casing commercial centrifugal pumps shown in Figure 5 were selected for the experimental assessment. Their respective back cover plate and impeller design gives better understanding of the actual rear axial clearance, act_cl . The design and geometrical parameters of the pumps are tabulated in Table 1. Based on the geometry of the *actuator*, specifically tailored clearance-reducing rings were used to minimize the clearance, as shown in Figure 6. Simple joint assemblies were used to attach these rings to the back cover plate of the corresponding pumps. The shapes of the clearance-reducing rings were a tapered ring, a hollow disk, and a cylindrical ring for $N_s = 19, 34, 54$ respectively. By applying the cavity filling ring, the clearance (cl) was reduced to the minimum feasible clearance gap of 1 mm, which is termed as no clearance, no_cl , for further analysis. The schematic view of the act_cl and no_cl cases are depicted in Figure 7.

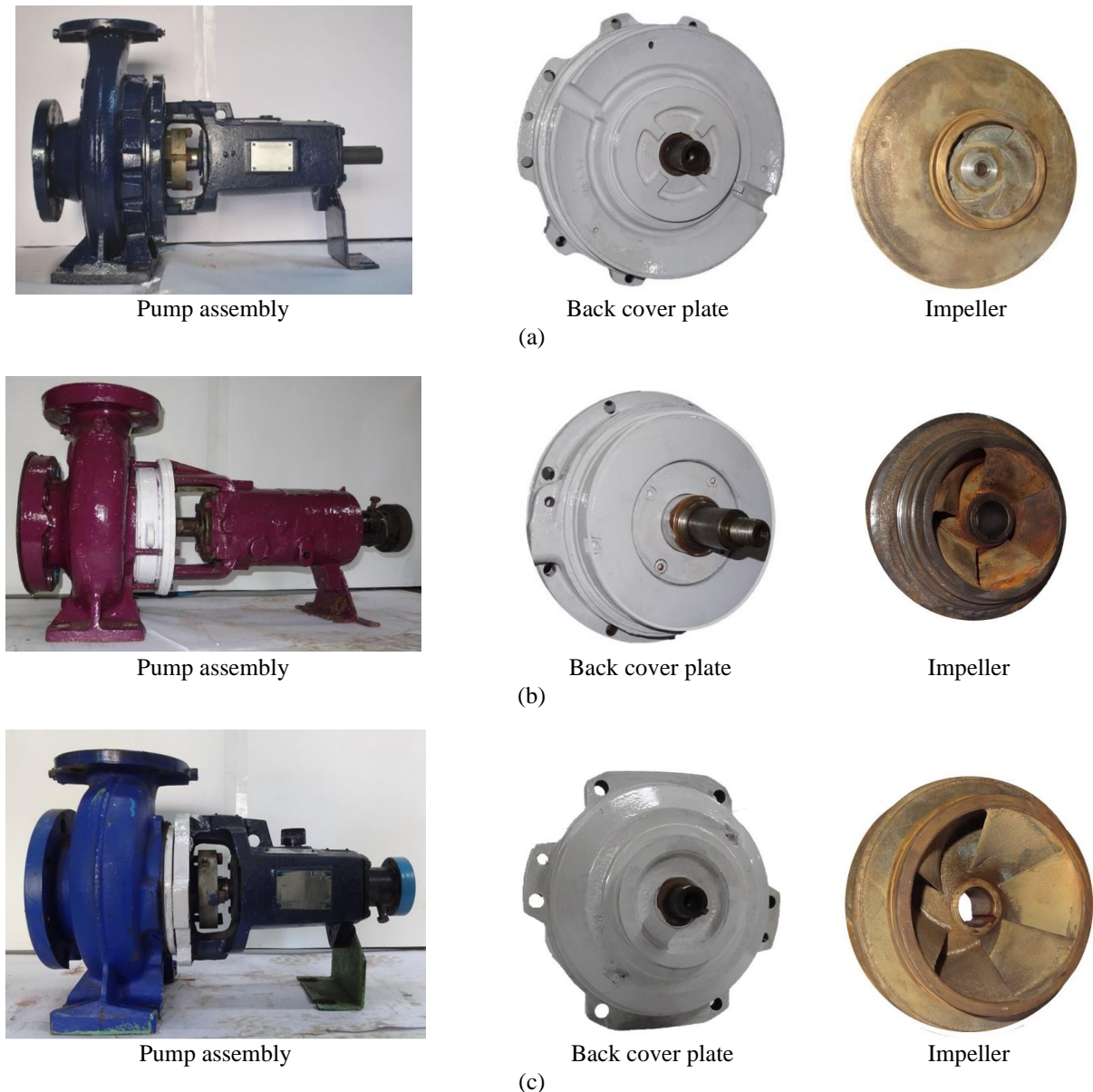


Figure 5. Commercial centrifugal pumps: (a) $N_s = 19$ rpm, (b) $N_s = 34$ rpm and (c) $N_s = 54$ rpm

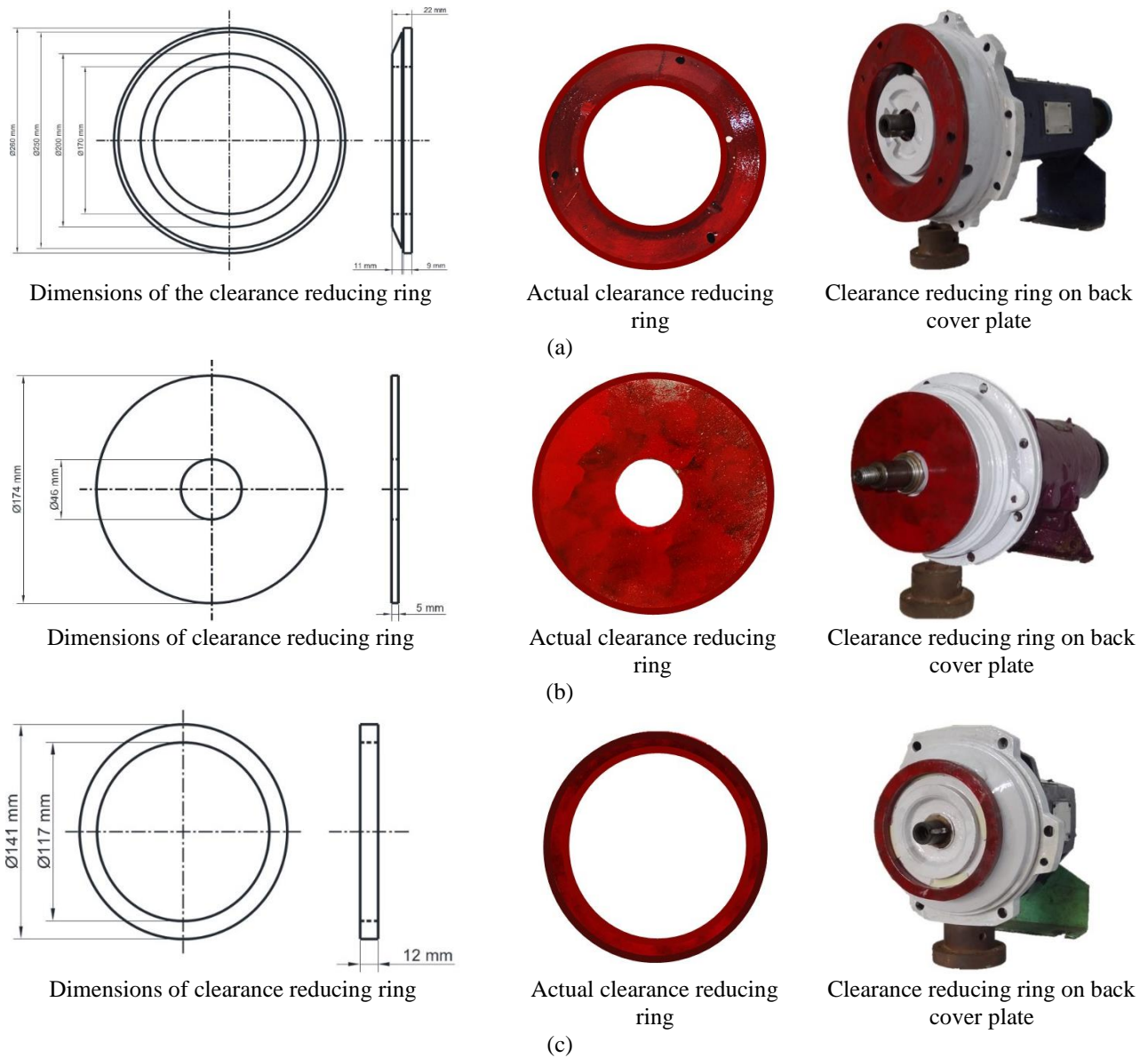


Figure 6. Clearance reducing ring for: (a) $N_s = 19$ rpm, (b) $N_s = 34$ rpm and (c) $N_s = 54$ rpm

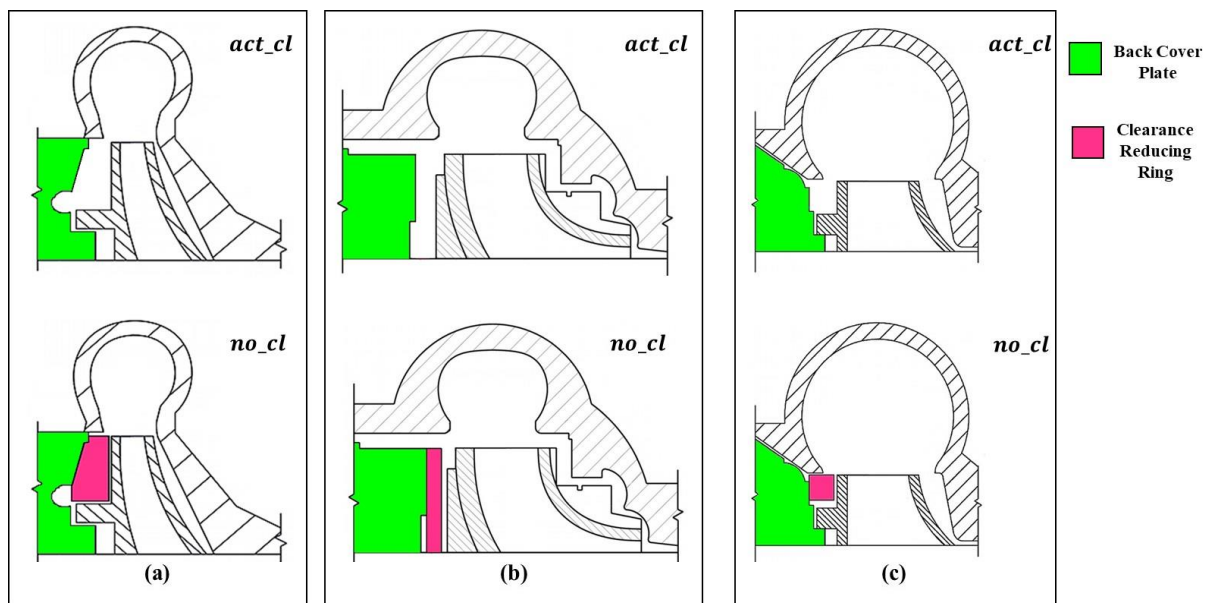


Figure 7. Schematic view of the *act_cl* and *no_cl* case for: (a) $N_s = 19$ rpm, (b) $N_s = 34$ rpm and (c) $N_s = 54$ rpm

Table 1. Design and geometrical parameters of the pumps

Parameter	Pump		
	$N_s = 19$	$N_s = 34$	$N_s = 54$
Head (H_d) in m	21.0	8.8	5.3
Flow rate (Q_d) in lps	17.5	13.8	16.8
Rotational speed (N_d) in rpm	1450	1450	1450
Blade number (Z_d)	5.0	5.0	6.0
Actual axial clearance (act_cl) in mm	24-14	7.0	13.0
Impeller inner radius (R_1) in mm	100.0	55.0	47.7
Impeller outer radius (R_2) in mm	130.0	87.0	70.5
Impeller outer width (B) in mm	15.5	22.0	27.0

2.2 Hydraulic Test Rig and Experimental Methodology

The hydraulic test bench setup utilized in the present experimental work is similar to that previously used by the authors, Dokiparti et al. [26], and is schematically depicted in Figure 8. As the setup used was open-loop, fluids did not heat up, and no temperature control system was required. A series of experimental tests has been conducted at the Fluid Mechanics and Fluid Machine Laboratory, Sardar Vallabhbhai National Institute of Technology, Surat, Gujarat, India (21.1663° N, 72.7833° E). The working fluid stored in the sump was water at 25 °C. Two different pressure transmitters were used to measure the inlet and outlet pressure with an accuracy of $\pm 0.065\%$. An electromagnetic flow meter having an accuracy of $\pm 0.5\%$ was employed to measure the flow rate range. Rotary torque sensor measures the required input torque with the accuracy of $\pm 0.25\%$. Each pump was driven by a variable frequency drive (VFD) unit connected to the electrical motor of the pump, allowing for rotation adjustment and fluid control. To regulate the line pressure and fluid flow rates, a control gate valve was used. The experimental setup utilized a Supervisory Control and Data Acquisition (SCADA) System for real-time data acquisition and automatic control. The SCADA system integrates multiple hardware and software components to ensure seamless operation. The hardware comprises sensors, relays, and switches that collect data, while the SCADA software processes and interprets this data, providing operators with meaningful insights. Additionally, it facilitates control operations and triggers alarms when necessary. A key component of the system is the PLC, an industrial computer responsible for receiving, processing, and transmitting data. The PLC gathers real-time measurements from various instruments, including head, flow rate, torque, and rpm, converting them into digital signals for further analysis. The processed data is then relayed to a central Human Machine Interface (HMI), which serves as the primary monitoring and control platform. The HMI enables operators to assess and manage all data from networked devices and sensors efficiently. The acquired data is systematically stored in a Microsoft Excel file format for record-keeping and further analysis.

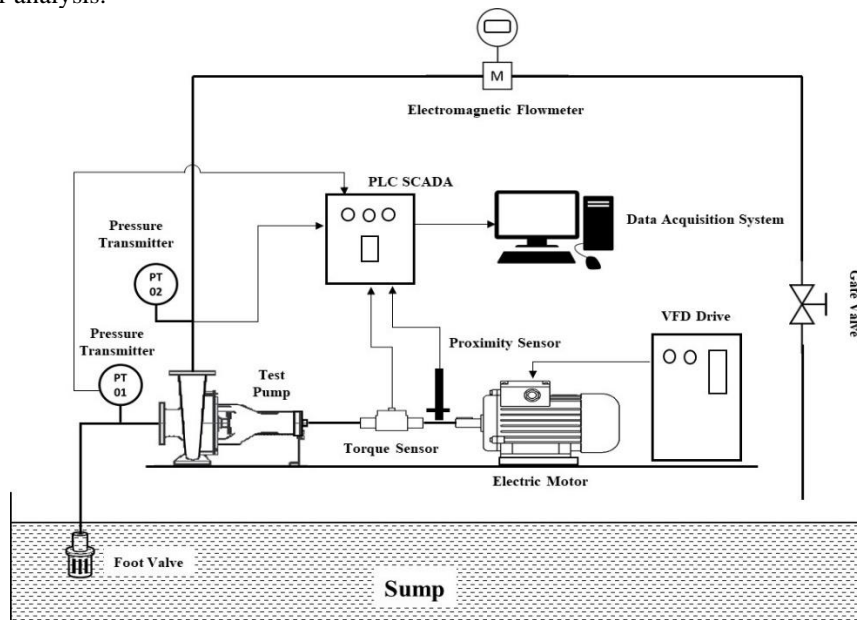


Figure 8. Schematic diagram of the hydraulic test setup

Moreover, an automatic feedback control system is integrated within the setup, allowing precise regulation of the test pump's operating conditions. Through the HMI, the pump can be controlled to maintain a constant speed, head, or flow rate, ensuring stability and accuracy in experimental observations. The flowmeter (Endress+Hauser-Promag 10 make) and pressure transmitters (Honeywell/ST-700 make) were calibrated by comparing it using a standard temperature/electrical calibrator as well as a pressure calibrator. In contrast, torque sensor (Honeywell-1703 make) was

calibrated against a dead weight torque test rig with calibrated lever arm and SS force weights. All the instruments were calibrated using the standard calibration methods at NABL accredited Enpro Enviro Tech and Engineers Pvt. Ltd. and Precise Calibration Lab, India. Considering the various operating range of all pumps, the common maximum flow rate taken were $Q_{max} = 16$ lps for design condition, while $Q_{max} = 11$ lps for off-design condition. The minimum flow rate was taken as $Q_{min} = 5$ lps as per the feasibility of the test setup using the manufacturer's pump data for both conditions. The average value of measured hydraulic performance parameters (H_T , T_{in} and η_o) were considered for further analysis. The variation in in performance parameters between *act_cl* and *no_cl* were evaluated and compared at both design conditions.

3. RESULTS AND DISCUSSION

Figure 9 shows the performance characteristic curves for $N_s = 34$ and $N_s = 54$ rpm at design condition, respectively. The initial interpretation of curves at design conditions indicates that the performance enhancement for the *no_cl* condition is compared to the *act_cl* over the whole range of flow rates. The performance parameters obtained for $N_s = 54$ were $H_T = 5.42$ m, $T_{in} = 6.67$ N·m and $\eta_o = 84.48\%$, while for $N_s = 34$ these values were $H_T = 8.30$ m, $T_{in} = 11.50$ N·m and $\eta_o = 70.31\%$ at Q_{max} . Although, the highest performance was obtained for $N_s = 54$, the best enhancement in performance parameters due to *cl* reduction was found for $N_s = 34$. Figure 10 represents the variation in performance parameters H_T , T_{in} and η_o due to *no_cl* at design condition. For $N_s = 34$, the improvement found at Q_{max} was $\Delta H_T = 0.55$ m (\uparrow), $\Delta T_{in} = 0.08$ N·m (\downarrow) and $\Delta \eta_o = 5.20\%$ (\uparrow), while these values for $N_s = 54$ were $\Delta H_T = 0.05$ m (\uparrow), $\Delta T_{in} = 0.05$ N·m (\downarrow) and $\Delta \eta_o = 1.42\%$ (\uparrow).

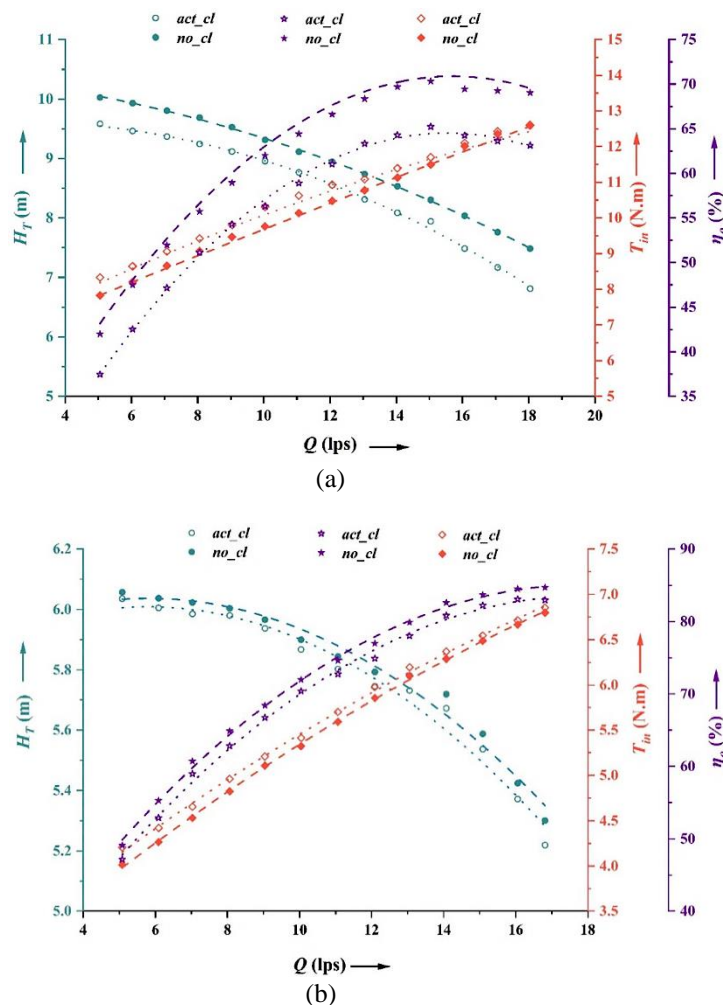


Figure 9. Performance characteristic curves at design condition for: (a) $N_s = 34$ and (b) $N_s = 54$

Similarly, the characteristic curves for $N_s = 19$, $N_s = 34$ and $N_s = 54$ at off-design condition are depicted in Figure 11(a), (b) and (c) respectively, while Figure 12(a), (b) and (c) represents variation in performance parameters H_T , T_{in} and η_o due to *no_cl*. Unlike the design condition, the highest improvement and change in performance parameters were observed for $N_s = 34$. The performance parameters obtained at Q_{max} were $H_T = 9.69, 3.93, 2.58$ m, $T_{in} = 15.14, 6.12, 3.25$ N·m and $\eta_o = 66.22, 66.49, 57.50\%$ for $N_s = 19, N_s = 34$ and $N_s = 54$ respectively. Also, the enhancement in performance found was $\Delta H_T = 0.26, 0.28, 0.06$ m (\uparrow), $\Delta T_{in} = 0.06, 0.15, 0.02$ N·m (\downarrow) and $\Delta \eta_o = 2.00, 6.20, 1.56\%$ (\uparrow) for $N_s = 19, N_s = 34$ and $N_s = 54$ respectively.

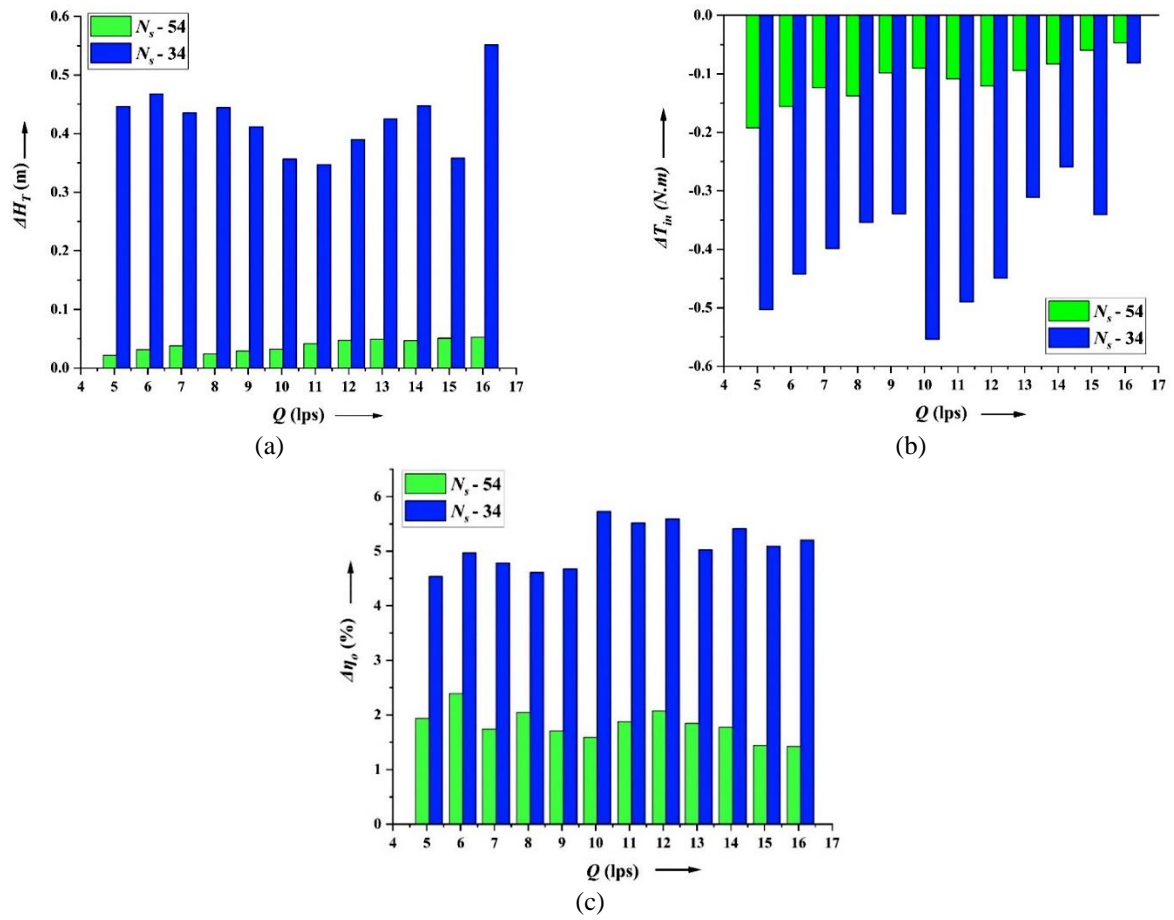


Figure 10. Performance enhancement at design condition of: (a) ΔH_T , (b) ΔT_{in} and (c) $\Delta \eta_o$

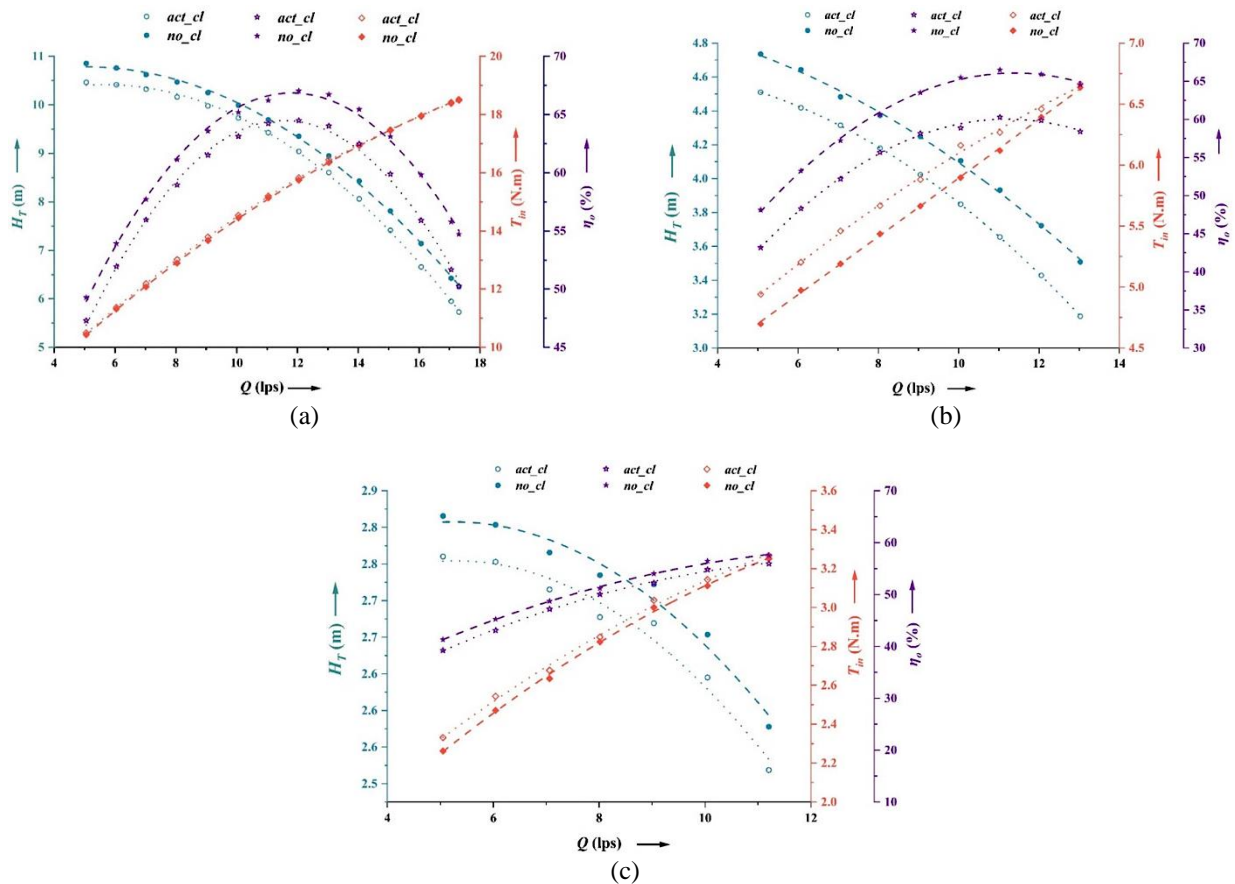


Figure 11. Performance characteristic curves at off-design condition for: (a) $N_s = 19$, (b) $N_s = 34$ and (c) $N_s = 54$

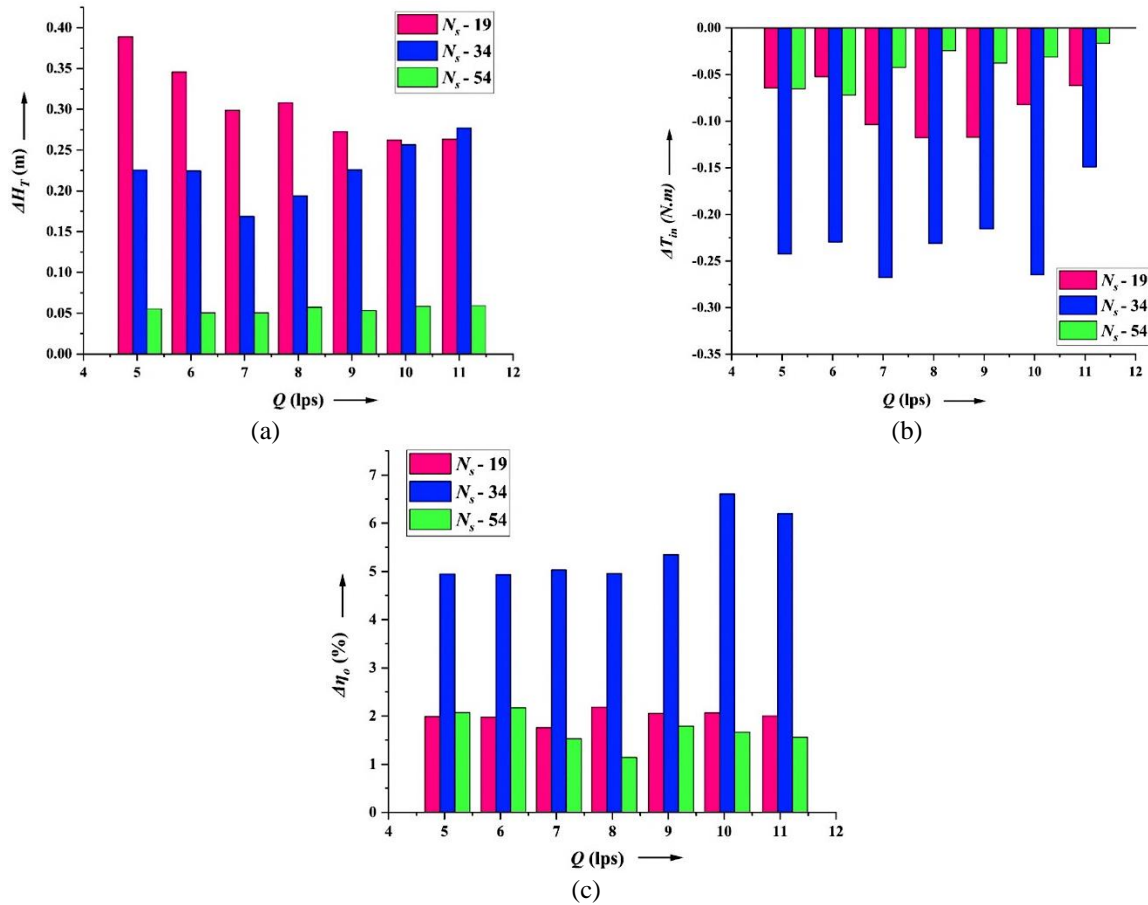


Figure 12. Performance enhancement at off-design condition of: (a) ΔH_T , (b) ΔT_{in} and (c) $\Delta \eta_o$

The enhancement in *no_cl* case compared to the *act_cl* can be understood as: In the *act_cl* case, clearance flow at the impeller entrance generates the high-speed leakage to strike with low-speed mainstream. This collision results in vortices and generates the reverse flow. This flow reversal obstructs the free flow of the impeller and increases the input T_{in} . In addition, the formation of these vortices disrupts the operation of the pump near the fluid mixing zone, creating more energy loss. While in *no_cl* case, lower clearance restricts the re-entrance of the fluid in the volute reduces the flow separation and maintains the more uniform smooth flow reducing the input T_{in} . Also, reduction in recirculation of fluid imparts more efficient transfer of hydraulic energy from the impeller leading to the improved H_T . These increment in H_T and decrement in T_{in} , ultimately enhances the η_o .

To gain a better understanding of performance improvement due to *cl* variation, consider the change in experimental disk friction head loss, ΔH_{T_L} was estimated using below equation:

$$\Delta H_{T_L} = [(H_{T_L})_{act_cl} - (H_{T_L})_{no_cl}] \tag{1}$$

where,

$$(H_{T_L})_{act_cl \text{ or } no_cl} = (H_{T_max})_{act_cl \text{ or } no_cl} - (H_T)_{act_cl \text{ or } no_cl} \tag{2}$$

$$(H_{T_max})_{act_cl \text{ or } no_cl} = \frac{(T_{in})_{act_cl \text{ or } no_cl} \times \omega}{\rho g Q} \tag{3}$$

Using the Eq. (1), the ΔH_{T_L} was calculated and plotted against the common flow rate range for all pumps at both design and off-design conditions, as shown in Figures 13 and 14, respectively. Over the entire operating range at design conditions, the average ΔH_{T_L} found was 1.0909 m and 0.2426 m for $N_s = 34$ and $N_s = 54$ respectively. Similarly, the average ΔH_{T_L} was 0.4771 m, 0.7030 m and 0.1492 m for $N_s = 19$, $N_s = 34$ and $N_s = 54$, respectively. The maximum ΔH_{T_L} implies less energy loss due to disk friction and more efficient conversion of kinetic energy into pressure energy in the form of H_{T_L} . In this regard, the best enhancement in performance parameters was obtained for $N_s = 34$ in compare to the $N_s = 54$ at design condition, while in off-design condition it was in order of $N_s = 34$ followed by $N_s = 19$ and $N_s = 54$. Also, the hollow disc shape of cavity filling ring in $N_s = 34$ allow less entrapment of fluid in clearance region compared to the tapered ring in $N_s = 19$ and cylindrical in $N_s = 54$ (see Figure 7). Because the hollow disk better seals the gap between the impeller and the volute, it probably produces a more effective barrier against fluid recirculation. A bigger and more constant surface area in contact with the fluid may be provided by this design, which would lessen the chance of high-pressure fluid escaping back into the low-pressure section. Furthermore, the hollow disk might offer a more

consistent and steady flow pattern, reducing energy losses and turbulence. This improves the fluid's entrapment within the intended flow route, transferring more of the impeller's energy to the fluid and raising the pump's total hydraulic efficiency.

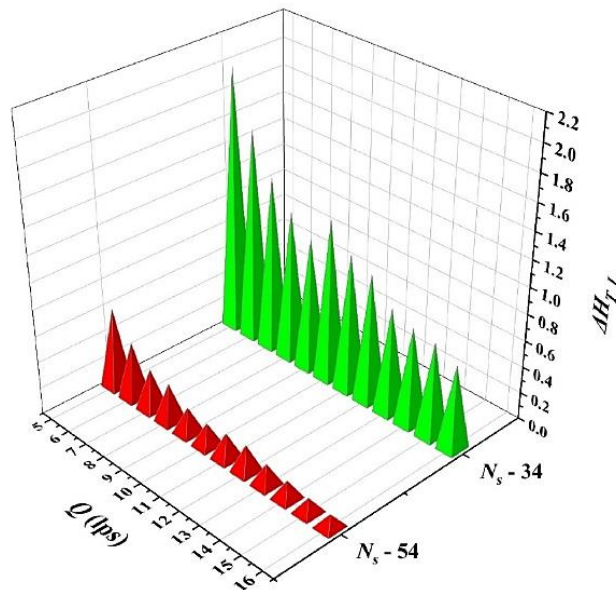


Figure 13. Change in experimental disk friction head loss (ΔH_{T-L}) at design condition for $N_s = 34$ and $N_s = 54$

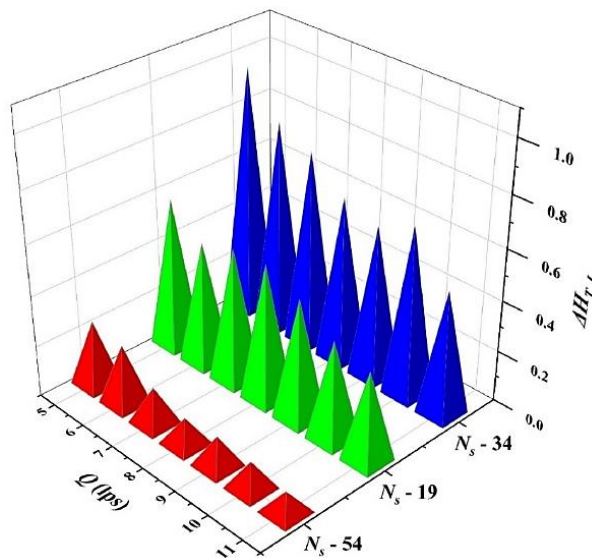


Figure 14. Change in experimental disk friction head loss, ΔH_{T-L} at off-design condition for $N_s = 19$, $N_s = 34$ and $N_s = 54$

The pump's on-field performance will determine the actual energy consumption and efficiency, contingent on-site conditions. Selecting the ideal pump requires being able to predict these performance characteristics. This article demonstrates how pump selection affects the energy consumption and efficiency of systems, and in turn, their cost-saving potential. The economic analysis of both conditions was done to evaluate the cost savings in *no_cl* compared to the *act_cl*. The standard maximum operating hours of each pump were taken as 300 days per year, assuming a constant head and flow rate, as per the manufacturer's data. Additionally, the electricity tariff was set at \$0.147/kWh [27]. Using the power generated due to increase in head, P_{gen} , the operating cost of the pump was calculated as below and the cost savings analysis is represented in Table 2.

$$Cost = P_{gen} \times \text{no. of operating days per year} \times 24 \times \text{electricity tariff} \tag{4}$$

From Table 2, it is easily obvious that the highest cost savings can be obtained in $N_s = 34$ at design condition compared to the other pumps. Additionally, this clearance-reducing ring may be the pinnacle of the pump industry revolution, given the number of pumps running concurrently.

Table 2. Cost savings analysis

Operating Condition	Pump	P_{gen} (kW)		Cost (\$)		Cost Savings (\$)
		<i>act_cl</i>	<i>no_cl</i>	<i>act_cl</i>	<i>no_cl</i>	
Design	$N_s - 34$	1.18	1.27	1248.69	1340.46	91.77
	$N_s - 54$	0.85	0.85	895.86	904.81	8.95
Off-Design	$N_s - 19$	1.02	1.05	1081.08	1110.36	29.29
	$N_s - 34$	0.40	0.43	418.54	450.61	32.07
	$N_s - 54$	0.28	0.28	293.57	300.25	6.68

4. CONCLUSIONS

An experimental analysis of three commercial centrifugal pumps ($N - s = 19, 34,$ and 54 rpm) was conducted to investigate the effect of reducing DF_L . Two different cases *act_cl* and *no_cl* were investigated at design and off-design conditions at various flow rates. The economic analysis is also presented to provide an economic perspective on the modification. The following concluding remarks have been made:

- i) In comparison of *act_cl*, *no_cl* exhibits a significant performance improvement in both the methods. In *no_cl*, the reverse clearance flow was restricted leading to the less entrapment and more uniform pattern fluid flow increases the conversion rate of kinetic energy to pressure energy. This efficient conversion improves H_T and η_o for all the rpms over a range of flow rate, while reduces the required input T_{in} .
- ii) At both design and off-design conditions, the $N_s = 34$ shows the highest enhancement in performance parameters in compared to $N_s = 19$ and $N_s = 54$ at *no_cl*. This is mainly due to the shape of the cavity filling ring utilised in $N_s = 34$. The hollow disk ring in $N_s = 34$ allows for the least entrapment of fluid in the clearance, providing a more constant flow pattern. Also, the $\Delta H_{T,L}$ due to disk friction was higher for $N_s = 34$ imparting more efficient energy transfer to the fluid.
- iii) The $\Delta H_{T,L}$ This approach allows for a more accurate representation of the pump's performance after modification and provides a robust framework for predicting the benefits of similar modifications in other pump systems. The revised equations are critical in understanding how reducing inefficiencies in the non-flow zone can lead to substantial performance gains, thus offering valuable insights for future pump design and optimization efforts.

This study highlights the potential for significant energy savings and performance improvements in centrifugal pumps by reducing disk friction losses through modifications to clearance space. Given the extensive use of pumps across industrial and domestic sectors, implementing such design modifications at a larger scale could lead to revolutionary advancements in energy efficiency. Future research could focus on further optimizing cavity-filling geometries, exploring advanced materials with lower friction factors, and evaluating the long-term durability and economic feasibility of such modifications. These advancements will pave the way for more sustainable and energy-efficient pumping systems, aligning with global efforts to reduce energy consumption and carbon emissions.

ACKNOWLEDGEMENTS

The authors sincerely acknowledge the support from the Sardar Vallabhbhai National Institute of Technology, Surat, and the Sarvajanik College of Engineering & Technology, Surat. The authors are also thankful to Mr. Sivadasan, Mr. Pruthviraj Solanki, and Mayank Patel for their contributions toward the development of the test rig and experimental work. This study was not supported by any grants from funding bodies in the public, private, or not-for-profit sectors.

CONFLICT OF INTEREST

The authors declare no conflicts of interest. There are no known competing financial interests or personal relationships that could be perceived as influencing the work reported in this paper. This paper has not been previously published, is not currently under review by any other journal, and will not be submitted elsewhere until this journal has made a decision.

AUTHORS CONTRIBUTION

D. Satish (Experimentation; Methodology; Validation; Investigation; Analysis; Writing - Original Draft; Review and Editing)

A. Doshi (Conceptualization; Methodology; Investigation; Resources and Supervision)

M. Bade (Methodology; Investigation; Resources and Supervision)

AVAILABILITY OF DATA AND MATERIALS

The data supporting this study's findings are available on request from the corresponding author.

ETHICS STATEMENT

Not applicable

REFERENCES

- [1] IEA, “International energy outlook 2023 with projection to 2025,” International Energy Agency, 2023 [Online]. Available: <https://www.iea.org/reports/world-energy-outlook-2023>
- [2] European Commission, “Ecodesign design for water pump,” *Official Journal of the European Union*, vol. 165, no. 547/2012, pp. 28-36, 2012.
- [3] H. Ahmed, S. Electric, J. Creamer, “Why pumping infrastructure matters,” Empowering Pumps & Equipment, 2017 [Online]. Available: <https://empoweringpumps.com/schneider-electric-pumping-infrastructure-matters/>
- [4] J. F. Gülich. Centrifugal Pumps. 4th Ed. Springer International Publishing, 2019.
- [5] J. F. Gülich, “Disk friction losses of closed turbomachine impellers,” *Engineering Research*, vol. 68, no. 2, pp. 87–95, 2003.
- [6] M. M. Raheel, A. Engeda, “Systematic design approach for radial blade regenerative turbomachines,” *Journal of Propulsion and Power*, vol. 21, no. 5, pp. 884–892, 2005.
- [7] H. W. Iversen, “Performance of the periphery pump,” *Journal of Fluids Engineering*, vol. 77, no. 1, pp. 19–22, 1955.
- [8] M. Shimosaka, “Research on the characteristics of regenerative pump,” *Transactions of the Japan Society of Mechanical Engineers*, vol. 25, no. 157, pp. 951–959, 1959.
- [9] W. C. Choi, I. S. Yoo, M. R. Park, M. K. Chung, “Experimental study on the effect of blade angle on regenerative pump performance,” *Proceedings of the Institution of Mechanical Engineers, Part A: Journal of Power and Energy*, vol. 227, no. 5, pp. 585–592, 2013.
- [10] A. Shirinov, S. Oberbeck, “High vacuum side channel pump working against atmosphere,” *Vacuum*, vol. 85, no. 12, pp. 1174–1177, 2011.
- [11] A. Shirinov, S. Oberbeck, “Optimisation of the high vacuum side channel pump,” in *7th International Conference on Compressors and Their Systems*, pp. 81–92, 2011.
- [12] H. Horiguchi, K. Wakiya, Y. Tsujimoto, M. Sakagami, S. Tanaka, “Study for the increase of micro regenerative pump head,” *International Journal of Fluid Machinery and Systems*, vol. 2, no. 3, pp. 189-196, 2009.
- [13] H. Sixsmith, “The theory and design of structures,” *Nature*, vol. 92, no. 2288, pp. 4–4, 1913.
- [14] M. Badami, “Theoretical and experimental analysis of traditional and new periphery pumps,” *SAE Technical Papers*, p. 971074, 1997.
- [15] B. C. Will, F. K. Benra, H. J. Dohmen, “Investigation of the flow in the impeller side clearances of a centrifugal pump with volute casing,” *Journal of Thermal Science*, vol. 21, no. 3, pp. 197–208, 2012.
- [16] A. F. Ayad, H. M. Abdalla, A. A. El-Azm Aly, “Effect of semi-open impeller side clearance on the centrifugal pump performance using CFD,” *Aerospace Science and Technology*, vol. 47, pp. 247–255, 2015.
- [17] L. Cao, Y. Zhang, Z. Wang, Y. Xiao, R. Liu, “Effect of axial clearance on the efficiency of a shrouded centrifugal pump,” *Journal of Fluids Engineering*, vol. 137, no. 7, p. 071101, 2015.
- [18] H. Pehlivan, Z. Parlak, “Investigation of parameters affecting axial load in an end suction centrifugal pump by numerical analysis,” *Journal of Applied Fluid Mechanics*, vol. 12, no. 5, pp. 1615–1627, 2019.
- [19] S. Adistiya, A. T. Wijayanta, “Effect of clearance gap on hydraulic efficiency of centrifugal pump,” in *AIP Conference Proceedings*, vol. 2097, p. 030053, 2019.
- [20] L. Zheng, X. Chen, H.S. Dou, W. Zhang, Z. Zhu, X. Cheng, “Effects of clearance flow on the characteristics of centrifugal pump under low flow rate,” *Journal of Mechanical Science and Technology*, vol. 34, no. 1, pp. 189–200, 2020.
- [21] Y. Inaba, K. Sakai, K. Miyagawa, M. Iino, T. Sano, “Investigation of flow structure in a narrow clearance of a low specific speed centrifugal impeller,” *Journal of Fluids Engineering, Transactions of the ASME*, vol. 143, no. 12, p. 121109, 2021.
- [22] F. Jin, N. Li, Z. Wei, Y. Wu, R. Tao, R. Xiao, “Sensitivity analysis on the influence factors of clearance axial force of a varying-speed centrifugal pump,” *Journal of Physics: Conference Series*, vol. 2217, no. 1, p. 012001, 2022.
- [23] G. Peng, S. Hong, H. Chang, F. Fan, Y. Zhang, P. Shi, “Numerical and experimental research on the influence of clearance between impeller and cover on the pump performance,” *Mechanika*, vol. 28, no. 1, pp. 67–72, 2022.
- [24] B. Kim, M. H. Siddique, S. A. I. Bellary, A. S. Aljehani, S. W. Choi, D. E. Lee, “Investigation of a centrifugal pump for energy loss due to clearance thickness while pumping different viscosity oils,” *Results in Engineering*, vol. 18, p. 101038, 2023.

- [25] S. Maeda, T. Sano, K. Miyagawa, K. Sakai, "Reduction of disk friction loss by applying a fin to the back of a centrifugal impeller," *Journal of Fluids Engineering*, vol. 146, no. 7, p. 071107, 2024.
- [26] S. Dokiparti, A. Doshi, M. H. Bade, "Centrifugal pump performance improvement using back cavity filling," *Physics of Fluids*, vol. 36, no. 6, p. 067129, 2024.
- [27] M. Rossi, G. Comodi, N. Piacente, M. Renzi, "Energy recovery in oil refineries by means of a hydraulic power recovery turbine (HPRT) handling viscous liquids," *Applied Energy*, vol. 270, p. 115097, 2020.